

Two Frequency Estimation Schemes Operating Independently of Timing Information

Ferdinand Classen and Heinrich Meyr

Aachen University of Technology, ISS, Templergraben 55, 52056 Aachen, Germany
Telephone +49-241-807884, Fax +49-241-807631, email: classen@ert.rwth-aachen.de

Abstract

In this contribution we propose two novel carrier frequency estimation schemes which are well suited for a fully digital receiver. Both algorithms are able to cope with frequency offsets in the range of 100% and more without requiring that clock synchronization has to be performed in advance or that known symbols are available. We analyze and compare their performance in terms of their acquisition speed as well as in terms of the estimation error mean and variance. Computer simulations are used to verify the analysis.

1 Introduction

Fully digital implementation of receivers in which no feedback from digital to analog parts of the receiver exists is one of the major trends in transmission system design. This has highlighted the critical issue of carrier recovery particularly in cases where the frequency offset $\Omega_0 T$ takes large values $|\frac{\Omega_0 T}{2\pi}| \approx 100\%$ and where the frequency synchronization must be established within a fixed time period determined by the transmission system specifications. Several authors [1–4] have investigated various types of approaches to frequency synchronization algorithms. Common to all the works, is the fact that the algorithms need timing information. But at the beginning of the transmission, timing is not available and it is mandatory to operate independently of a clock recovery scheme.

In this paper, we are concerned with the problem of estimating a frequency offset if neither timing nor known data are available. For this reason the algorithms we present operate in a, so called, *non data aided* and *non timing directed* (NDA NεD) mode. Both the acquisition as well as the tracking performance serves as a quality measure.

Before we discuss the algorithms, we shortly address the problem of the analog prefilter and the choice of the sampling rate. As mentioned above, we assume that no tuning of the mixer unit in front of the analog prefilter is possible. Therefore, the analog prefilter has to be selected in such a way that the signal (frequency shifted by $\Omega_0 T$) can pass the analog prefilter without any distortion. In order to simplify the discussion we assume that the analog prefilter is an ideal low pass filter of bandwidth $B_f = \frac{1}{2T_s}$ and that the received signal can be written as

$$\begin{aligned} r(kT_s) &= e^{j(\Omega_0 kT_s + \theta_0)} \sum_n a_n g(kT_s - nT - \varepsilon_0 T) + n(kT_s) \\ &= s(kT_s, \{\Omega, \theta, \varepsilon, \mathbf{a}\})_{|\{\Omega_0, \theta_0, \varepsilon_0, \mathbf{a}_0\}} + n(kT_s) \end{aligned} \quad (1)$$

where

- $\{a_n\}$ is a sequence of M-PSK data symbols with $|a_n|^2 = 1$,
- $g(t)$ is the impulse response of the convolution of the transmitted pulse with the channel impulse response and the analog prefilter (square root raised cosine with excess bandwidth β and energy normalized to unit)
- T is the symbol duration and T_s is an appropriate sampling time (e.g. $T_s = T/4$)
- $n(kT_s)$ is a complex-valued Gaussian noise process with statistically independent real and imaginary parts each having a variance of $\sigma^2 = \frac{N_0}{2} \frac{T}{T_s}$. Note that, the of the analog prefilter is assumed to be $2B_f = \frac{1}{T_s}$,
- θ_0 is the unknown initial phase shift
- ε_0 is the unknown initial timing offset
- Ω_0 is the unknown slowly varying frequency offset

Following the above consideration, the maximal frequency offset any structure can cope with is upperbounded by

$$|\Omega_{0, max}| \leq B_f - \frac{1}{2T} (1 + \beta) \quad (2)$$

One of the two frequency estimation structures to be presented is able to handle such a frequency offset. Be aware that $|\Omega_{0, max}|$ depends only on the sampling rate and the appropriate shaping of the analog prefilter.

The derivation of the algorithms is based on the attempt to maximize the loglikelihood function

$$\Lambda(r_f(kT_s) | \Omega, \theta, \varepsilon, \mathbf{a}) = \sum_{k=-\infty}^{k=\infty} \text{Re}\{r(kT_s) s^*(kT_s)\} \quad (3)$$

or a suitable approximation to it [1, 5]. ($\Lambda(\cdot | \Omega, \theta, \varepsilon, \mathbf{a})$ means that the function depends on $\{\Omega, \theta, \varepsilon\}$ as well as on $\{a_n\}$.) The first step in the derivation of an NDA NεD algorithm is to find an appropriate likelihood function (denoted by $\Lambda(r_f(kT_s) | \Omega)$) which has to be maximized in a second step. Note, that no other trial parameters than Ω may enter into $\Lambda(r_f(kT_s) | \Omega)$. It can be shown [5] that

$$\Lambda(r_f(kT_s) | \Omega) = \sum_{k=-\infty}^{k=\infty} |z(kT_s)|^2 \quad (4)$$

is an appropriate formulation, where $z(kT_s)$ is given by

$$z(kT_s) = ((r(lT_s) e^{-j\Omega lT_s}) \otimes g^*(-lT_s))_{kT_s} \quad (5)$$

and where \otimes means convolution. The performance of the algorithms is expressed in terms of the bias, the mean of the

estimation error $E\{\Omega_0 - \hat{\Omega}\}$, and its variance. Additionally, we introduce the value P_{miss} to denote the probability that the estimation error is larger than a given threshold Ω_{thres} . As we see below, self noise phenomena will strongly influence the tracking behavior. This influence can only be mitigated by increasing the estimation length, which is often not possible, since, particularly in TDMA applications or spontaneous packet transmission systems, a frequency estimate must be generated from a fixed set of received samples. Therefore, we understand NDA NeD algorithms as a part of a two stage synchronization scheme, whose task is to generate as fast as possible a coarse frequency estimate $\hat{\Omega}_{1stage}$. With the help of this estimate the synchronization schemes of the second stage should be able to lock.

The paper is organized as follows. The next two sections describe the algorithms and give an analysis of them. Section 4 summarizes and interprets the simulation results. The conclusions are drawn in section 5.

2 Non Timing Aided Frequency Error Detector

In this section we propose an NDA NeD frequency error detector (FED) suitable for automatic frequency control (AFC) loops. The derivation of the NeD FED starts from (4) and is very similar to that described in [1, 6], where the derivation of a timing directed FED (subsequently called ϵ D FED) is based on the maximization of the loglikelihood formulation

$$\Lambda(r_f(kT_s | \Omega, \epsilon)) = \sum_N |z(nT + \epsilon T, \Omega)|^2 \quad (6)$$

Keep in mind, that the FED in [1] needs timing information, because (6) depends on the timing parameter ϵ , whereas (4) does not. The resulting structure of the NDA NeD FED does not significantly differ from the NDA ϵ D FED of [1]. Therefore, we state only the major differences. The main difference is that the NeD FED outputs one error signal

$$u(lT_s) = \text{Re}\{z(lT_s) z_{FMF}^*(lT_s)\} \quad (7)$$

(with $z_{FMF}(lT_s) = [(r(kT_s)e^{-j\Omega kT_s}) \otimes ((j2\pi kT_s) g(kT_s))]_{lT_s}$) for each sampling instant, whereas the ϵ D FED of [1] generates only one error signal $u(nT)$ for every symbol period. The analysis of the above structure shows that the estimate

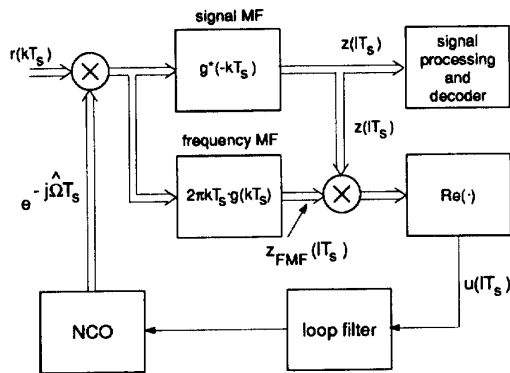


Figure 1: Block diagram of a NDA NeD frequency control loop

is unbiased provided data and noise are statistically independent. The slope of the s-curve in Fig. 2 is found to be

$$K_{\Omega\Omega} = \frac{\pi^2}{8\beta} \quad (8)$$

and is, as expected, independent of the timing shift ϵ_0 . As outlined in the introduction, the algorithm suffers from self noise. An analysis of the jitter caused by the self noise gives

$$\text{Var}\left(\frac{\hat{\Omega}T}{2\pi}\right) = \frac{T_{SXS}}{K_{\Omega\Omega}^2} (2B_L T) \quad (9)$$

where $2B_L T$ is the two sided noise bandwidth of the loop. We analyzed the factor $(T_{SXS}/K_{\Omega\Omega}^2)$ for different roll off factors and after lengthy calculation we found that this factor does not vary significantly with the roll off factor $T_{SXS}/K_{\Omega\Omega}^2 = 0.0157; 0.0255; 0.024$ for $\beta = 0.35; 0.5; 0.9$. From (9) it is clear that the self noise is proportional to the loop bandwidth. Figure 3 shows the simulated variance for different loop bandwidths. It is obvious that the self noise contribution (dashed line) becomes dominating for moderate and high SNR values. The frequency range the algorithm can cope

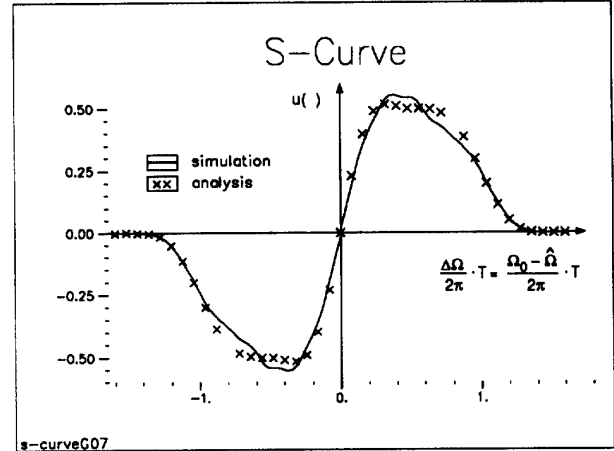


Figure 2: s-curve of the NDA NeD frequency control loop

with is exactly the same as that of [1] and is given by $|\Omega_{0,max}T| < 1 + \beta$.

Common to all feed back structures, the acquisition length depends on the amount of the frequency offset $|\Omega_0|$. The acquisition length L_{aq} can be assessed from a linearized model of the tracking loop where the frequency detector characteristic in Fig. 2 is linearized piecewise. In table 1 we have summarized the acquisition lengths, measured in required symbol intervals, for different loop bandwidths. The calculations and the simulation, respectively, were performed for an acquisition process in the noiseless case where the initial frequency offset was set to $\Omega_0 T / 2\pi = 1$ and we defined the acquisition process to be successfully ended if the difference between the estimated frequency offset and the true frequency offset $\Delta f T = \frac{1}{2\pi} |\Omega_0 T - \hat{\Omega} T|$ was

less than 0.01. These results should give only a rough guess about the order of magnitude of the length of the acquisition process. The exact analysis of the loop acquisition time requires more sophisticated mathematical tools mentioned in chapter 4 of [7].

$2B_L T$	$3.13 \cdot 10^{-2}$	$1.5 \cdot 10^{-2}$	$6 \cdot 10^{-3}$	$3.13 \cdot 10^{-3}$
L_{aq} (symbols)	150	300	747	1494

Table 1 Acquisition length L_{aq}

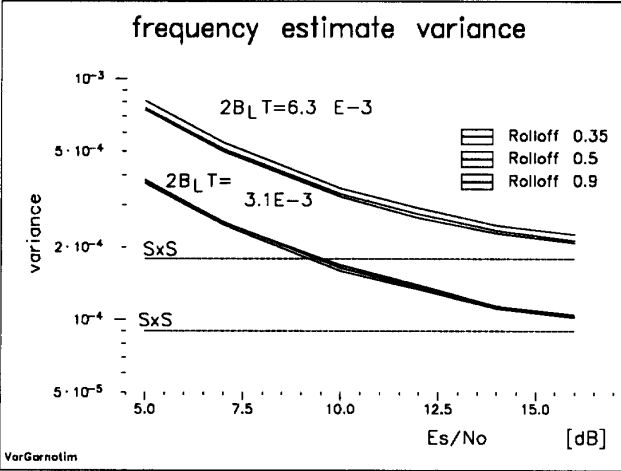


Figure 3: Simulated variance of the NDA NeD frequency control loop (QPSK transmission) dotted line: SxS part for $2B_L T = 1.5 \cdot 10^{-2}$ and $2B_L T = 3.12 \cdot 10^{-3}$ and $\beta = 0.5$

3 Direct Frequency Estimator

In this section we describe and analyze a so called *non data directed, non timing directed, feed forward* (NDA NeD FF) approach. Once again, we base the derivation of this algorithm on the maximum likelihood approach. We start from the likelihood function (3). In contrast to the estimators mentioned so far, the basic idea behind this algorithm is that the problem of frequency estimation can be reduced to the problem of estimating the phase of a complex phasor. Neglect for a moment the influence of the modulation in (1). We recognize that the phase process $\theta(kT_s) = \theta_0 + \Omega_0 kT_s$ is increased by an amount of $\Delta\theta = \Omega_0 T_s$ between two sampling instants. Averaging $\Delta\theta$ would provide an indication of Ω_0 .

Now let us conjecture the following approximation

$$s(kT_s, \mathbf{A}) \approx e^{j\Omega_0 kT_s} s((k-1)T_s, \mathbf{A}) \quad (10)$$

Obviously the larger the ratio T/T_s is the better this approximation becomes ($s(kT_s, \mathbf{A})$ is given by (1)). The maximum of (3) is reached in the noiseless case if the parameter set $\mathbf{A} = \{\Omega, \theta, \varepsilon, \{a\}\}$ of $s(kT_s, \mathbf{A})$ coincides with the true set

$\mathbf{A}_0 = \{\Omega_0, \theta_0, \varepsilon_0, \{a_0\}\}$ of $r(kT_s)$. A common high SNR approximation gives

$$s((k-1)T_s, \mathbf{A})|_{\mathbf{A}=\mathbf{A}_0} \approx r((k-1)T_s) \quad (11)$$

Inserting (10) and (11) into (3) gives

$$\Lambda_\Omega \approx \text{Re} \left\{ e^{-j\Omega T_s} |H| e^{+j \arg\{H\}} \right\} \quad (12)$$

with

$$H = \sum_{k=-\infty}^{k=\infty} r(kT_s) r^*((k-1)T_s) \quad (13)$$

Since the expression H is independent of the trial parameter Ω the maximum of (12) is obtained via

$$\hat{\Omega} T_s = \arg \left\{ \sum_{k=-\infty}^{k=\infty} r(kT_s) r^*((k-1)T_s) \right\} \quad (14)$$

At a first glance, we can conclude that we have found a very simple estimation rule, where neither a search operation nor any determination of the other elements of the parameter set $\mathbf{A}_0 = \{\theta_0, \varepsilon_0, \{a_0\}\}$ are required. But it remains to be proved that the estimate generated via (14) is appropriate in terms of

1. the expected variance and
2. the bias ($E\{\Omega_0 - \hat{\Omega}\} = 0$).

Before we proceed, an additional comment should be made on the estimation interval of (14). The estimation interval of (14) coincides with the observation interval of (3) which ranges from $-\infty$ to ∞ . Thus, we replace the unlimited observation interval by the finite estimation length denoted by L_F (measured in symbol periods) and now we can write (14) as

$$\hat{\Omega} T_s = \frac{T}{T_s} \arg \left\{ \sum_{(T/T_s) L_F} r(kT_s) r^*((k-1)T_s) \right\} \quad (15)$$

A block diagram of the estimator is shown in Fig. 4. First

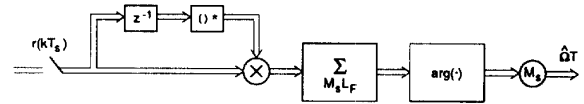


Figure 4: Block diagram of the direct estimator structure and $M_s = T/T_s$

of all, we have to show that the estimate is unbiased. In a second step we investigate the estimate variance.

The analysis of the estimator is impeded by the nonlinear argument operation. To overcome this problem we use the approach outlined in [8, 4]. This approach is based on the fact that the argument operation can be linearized if the

estimate variance is small. This is not a severe restriction since small variances are the only case of interest.

Following this approach, the expected value of $\hat{\Omega}$ can be shown to be

$$\hat{\Omega}T_s = \arg E \left\{ \sum_{L_F(T/T_s)} r(kT_s) r^*((k-1)T_s) \right\} \quad (16)$$

$$= \arg \left\{ e^{j\Omega_0 T_s} \left(L_F \frac{1}{T_s} h(-T_s) \right) \right\}$$

where $h(\cdot)$ is given by $h(kT_s) = (g(t) \otimes g^*(-t))|_{t=kT_s}$. Provided $h(\cdot)$ is real, which is fulfilled for example in case of a root raised cosine filter characteristic of the transmitter filter, the estimator (15) gives an unbiased estimate and is completely independent of the unknown parameters $\{\theta_0, \varepsilon_0, \{a_0\}\}$. Simulation results certified our assertion to be valid. For example, the mean $E\{(\Omega_0 - \hat{\Omega})T/2\pi\}$ calculated from the simulation results of 10.000 independent estimations was always less than 10^{-3} for a given SNR of $E_b/N_0 = 4\text{dB}$ and an estimation length of $L_F = 64$. Our next step is to analyze the estimate variance. It is favorable to use the following notation

$$\text{Var}\{\hat{\Omega}T\} = \sigma_{SxS}^2 + \sigma_{SxN}^2 + \sigma_{NxN}^2 \quad (17)$$

which reflects that the frequency jitter is caused by (signal x signal), (signal x noise) and (noise x noise) interactions. Using some approximations the variances can be calculated and we receive for BPSK and QPSK transmission the following set of formulas

1. (signal x signal) only for QPSK (for BPSK: $\sigma_{SxS} = 0$)

$$\sigma_{SxS} = \frac{(T/T_s)^2}{2(2\pi)^2 h^2(T_s)} \frac{1}{L_F} ((1 - (\beta/4)) - (I_1 + 2I_2)) \quad (18)$$

2. (signal x noise) for QPSK and BPSK

$$\sigma_{SxN} = \frac{(T/T_s)^2}{(2\pi)^2 h^2(T_s)} \frac{1}{L_F} (1 - h(2T_s)) \frac{1}{SNR} \quad (19)$$

3. (noise x noise) for QPSK and BPSK

$$\sigma_{NxN} = \frac{(T/T_s)}{2(2\pi)^2 h^2(T_s)} \frac{1}{L_F} \left(\frac{T/T_s}{SNR} \right)^2 \quad (20)$$

where I_1 is given by

$$I_1 = 2 \int_0^{(1+\beta)/2T} H^2(f) \cos(4\pi f T_s) df \quad (21)$$

and I_2 is given by

$$I_2 = \int_0^{(1+\beta)/2T} H(f) H(f+1/T) \sin(4\pi f T_s) df \quad (22)$$

(where $H(f)$ is the Fourier transform of $h(t) = g(t) \otimes g^*(-t)$). Figures 5 and 6 show some simulated variances for various estimation lengths and rolloff factors. The good agreement between analytically obtained curves and the simulation proves our approximations to be valid. Further simula-

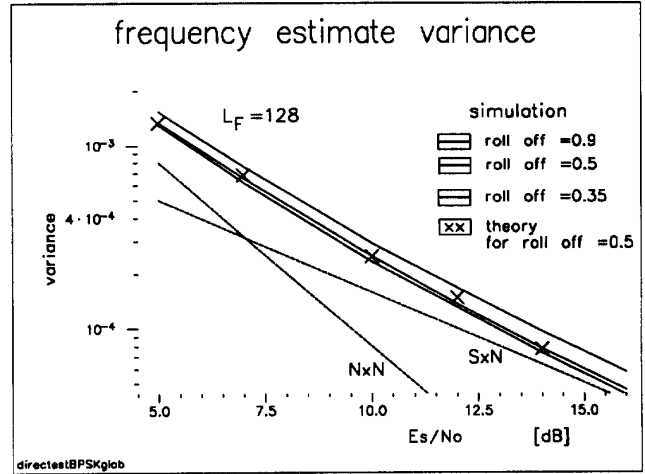


Figure 5: $\text{Var}(\hat{\Omega}T/2\pi)$ for BPSK transmission, $T/T_s = 4$, L_F estimation length
dotted lines: SxN, NxN -part for $L_F = 128$ and $\beta = 0.5$

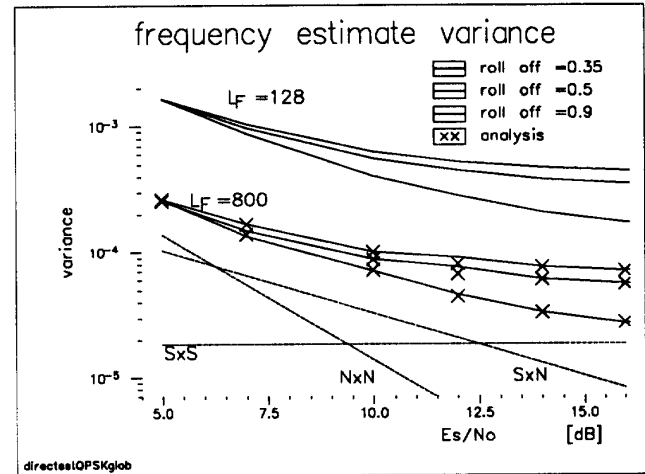


Figure 6: $\text{Var}(\hat{\Omega}T/2\pi)$ for QPSK transmission, $T/T_s = 4$, L_F estimation length
dotted lines: SxS, SxN, NxN -part for $L_F = 800$ and $\beta = 0.9$

tions, not reported here, verify that the estimate properties are independent of the parameter set $\{\theta_0, \varepsilon_0\}$, as expected from our theoretical considerations.

The maximum frequency offset Ω_{max} the estimator can cope with is upper bounded by $|\frac{\Omega_{max} T}{2\pi}| < \frac{T}{2T_s}$. However, even if the analog prefilter is optimally designed the permissible frequency offset is limited to (2). A last comment concerns the

behavior of the estimator if, instead of statistically independent data, periodic data pattern are transmitted. Simulation results show that the estimation properties remain untouched in the case that an unmodulated signal or a BPSK dotted signal ($a_m = (-1)^m$) is transmitted. This is an interesting result since the NDA N ϵ D feedback (FB) as well as the NDA ϵ D FB algorithm of [1] would fail in such cases.

4 Comparison and Interpretation

Both algorithms provide an unbiased frequency estimate. Therefore, we base our comparison on the assessment of the acquisition and tracking behavior. The acquisition length of the direct frequency estimator is doubtlessly given by the estimation length L_F and table 1 gives hints on the equivalent acquisition length L_{aq} of the NDA N ϵ D FB structure. In a scenario where a frequency synchronization has to be obtained from a fixed number of samples, the feedforward approach clearly outperforms the feedback approach because in terms of estimation error variance its estimate properties are much better than the FB results. We have seen that both algorithms suffer from self noise phenomena. The influence can only be mitigated by augmentation of the estimation interval. In many applications this is not feasible as well as undesirable. In such a case, the above algorithms should be understood as the first stage of a two stage synchronization scheme. In the first stage a coarse estimate should be generated as fast as possible using an NDA N ϵ D algorithm. The error of this one shot estimate $\left| \frac{\hat{\Omega} - \Omega_0}{2\pi} T \right|$ should be only with a low probability P_{miss} larger than a fixed threshold $\Omega_{threshold}$. The amount of this threshold is determined by the feasible pull in range of the algorithm employed in the second stage. In table 2 we summarized some simulation results for P_{miss} , assuming that $\Omega_{thres}T$ equals 12.5%. The simulations were performed for QPSK transmission and $\beta = 0.35$. As a rule of thumb, P_{miss} becomes very small (less than 10^{-5}) if the variance obeys $4.5 \sqrt{\sigma^2} < \frac{\Omega_{thres}T}{2\pi}$. This approximation is based on the assumption that the estimate error has an approximately Gaussian distribution with variance $E \left\{ \left(\frac{\hat{\Omega} - \Omega_0}{2\pi} T \right)^2 \right\} = \sigma^2$.

A last comment should be made about the algorithms employed in the second stage. Investigations not reported here show that once again the best choice are feed forward algorithms. It stands to reason that these algorithms make use of timing information, which should be available during the second stage, since it is safe to assume that timing sync can be established even in the presence of a carrier frequency offset of $|\Delta f T| \approx 12.5\%$ [9]. Such algorithms have the advantage that they do not suffer from self noise effects and that their variances decrease proportionally to $(1/L)^2$ or $(1/L)^3$ when L stands for their estimation length [4]. In addition, their structure is similar to that of the algorithm given by (16) which means that no extra hardware overhead is required.

L_F	4dB		7dB		10dB	
	σ^2	P_{miss}	σ^2	P_{miss}	σ^2	P_{miss}
64	4.5 E-3	6.7 E-2	2 E-3	5.2 E-3	1.2 E-3	1 E-4
128	2.2 E-3	8.0 E-3	9.9 E-4	1 E-4	6.2 E-4	< 1 E-4
256	1.1 E-3	1 E-4	5 E-4	< 1 E-4	3.1 E-4	< 1 E-4

Table 2 Variance $\text{Var} \left\{ \frac{\hat{\Omega} T}{2\pi} \right\} = \sigma^2$ and P_{miss} (QPSK transmission and $\beta = 0.35$)

5 Conclusion

We have presented two novel algorithms which are both well suited for carrier frequency synchronization in a fully digital receiver and which are able to cope with large frequency offsets in the range of $|\Omega_0 T| \approx 100\%$ and more. Both algorithms do not require the availability of timing information or known data. Our analysis and simulations show that the feed forward approach outperforms the feed back approach in terms of acquisition speed on condition that their tracking performance is comparable. Especially the direct frequency estimator can be recommended if frequency synchronization has to be performed within a fixed time period, as is commonly required in spontaneous packet transmission scenarios.

Bibliography

- [1] F. M. Gardner. "Frequency Detectors for Digital Demodulators Via Maximum Likelihood Derivation". *ESA-ESTEC Final Report: Part 2, ESTEC Contract No 8022-88-NL-DG*, March 1990.
- [2] Francis D. Natali. "AFC Tracking Performance". *IEEE COM*, COM-32(8):935-944, August 1984.
- [3] Thomas Albery and Volker Hespelt. "A new Pattern Jitter free Frequency Error Detector". *IEEE COM*, (2), Febr. 1989.
- [4] Ferdinand Classen, Heinrich Meyr and Philipp Sehier. "Maximum Likelihood Open Loop Carrier Synchronizer for Digital Radio ". *Proceedings ICC' 93*, pages 493-497, 1993.
- [5] H. Meyr et al. *Synchronization in Digital Communications Volume II*. to appear.
- [6] Aldo N. Andrea, and U. Mengali. "Performance of a Frequency Detector Based on the Maximum Likelihood Principle". *Proceedings Globecom 92*, pages 340-344, 1992.
- [7] H. Meyr and G. Ascheid. *Synchronization in Digital Communications*. John Wiley and Sons, Inc., New York London Sydney, 1989.
- [8] M. Oerder and M. Meyr. "Digital Filter and Square Timing Recovery". *IEEE COM*, (5):605-611, May 1988.
- [9] Ferdinand Classen, Heinrich Meyr and Philipp Sehier. "An All Feedforward Synchronization Unit for Digital Radio ". *Proceedings VTC' 93*, pages 738-741, 1993.